Case Studies in Thermal Engineering 31 (2022) 101810

Contents lists available at ScienceDirect

Case Studies in Thermal Engineering

journal homepage: www.elsevier.com/locate/csite

Exergy, sustainability and performance analysis of ground source direct evaporative cooling system

Gökhan Yıldız [a], Alper Ergün [b], Ali Etem Gürel [c], İlhan Ceylan [b], Ümit Ağbulut [c,*], Servet Eser [b], Asif Afzal [d,e], C.Ahamed Saleel [f]

[a] *Department of Mechanical Engineering, Institute of Graduate Studies, Duzce University, Duzce, Turkey*
[b] *Department of Energy Systems Engineering, Faculty of Technology, Karabuk University, Karabuk, Turkey*
[c] *Department of Mechanical Engineering, Faculty of Engineering, Duzce University, Duzce, Turkey*
[d] *Department of Mechanical Engineering, P. A. College of Engineering (Affiliated to Visvesvaraya Technological University, Belagavi), Mangaluru, 574153, India*
[e] *Department of Mechanical Engineering, School of Technology, Glocal University, Delhi-Yamunotri Marg, SH-57, Mirzapur Pole, Saharanpur District, Uttar Pradesh, 247121, India*
[f] *Department of Mechanical Engineering, College of Engineering, King Khalid University, PO Box 394, Abha, 61421, Saudi Arabia*

ARTICLE INFO

Keywords:
Evaporative cooling
Ground source
Exergy analysis
Sustainability
Energy consumption

ABSTRACT

A significant portion of global energy consumption is due to energy consumption in the buildings. Heating, cooling, and air conditioning systems have the largest share in this energy consumption. Evaporative cooling systems, which have the advantage of being economical, zero pollution, and easy maintenance are preferred to reduce energy consumption in buildings. These systems are used in many areas such as greenhouses, broiler houses, and warehouses. In this study, analyzes of exergy, sustainability, and cooling efficiency in four different situations of a ground source direct evaporative cooling system were made. The system was studied in four different cases. While the highest exergy efficiency was obtained in case 3 with 20.83%, the exergy efficiencies in other cases were obtained as 16.83%, 17.49%, and 18.36%, respectively. In addition, the highest specific exergy loss was determined as 100.51 J/kg in case 2, while it was calculated as 73.08 J/kg, 80.23 J/kg, and 73.05 J/kg for the other cases, respectively. It is seen that the sustainability values are in parallel with the exergy efficiency when the evaporative cooling system is examined for four different cases. The sustainability values were determined as 1.20 for case 1, 1.21 for case 2, 1.26 for case 3, and 1.22 for case 4. It is determined that the exergy efficiency gives precise information about the usability and sustainability of the system when these situations are evaluated. The exergetic improvement potential (EIP) was determined as 0.061 for case 1, 0.082 for case 2, 0.063 for case 3, and 0.059 for case 4, respectively. Although the highest exergy efficiency is obtained in case 3, it has a higher recovery potential than case 1 and case 4. In addition, cooling efficiencies for four different cases were obtained as 33.70%, 34.81%, 41.69%, and 36.95%, respectively. The temperature differences between the room and ambient temperatures were determined as 1.45 °C, 1.21 °C, 1.6 °C, and 1.48 °C for each case, respectively.

* Corresponding author.
E-mail address: umitagbulut@duzce.edu.tr (Ü. Ağbulut).

https://doi.org/10.1016/j.csite.2022.101810
Received 19 November 2021; Received in revised form 6 January 2022; Accepted 16 January 2022
Available online 19 January 2022

Nomenclature

c_p	Specific heat (kJ/kg.°C)
DEC	Direct evaporative cooling
IEC	Indirect evaporative cooling
EIP	Exergetic improvement potential
$\dot{Ex}$	Exergy (J)
ex	Specific exergy (J/kg)
h	Specific enthalpy (J/kg)
m	Mass (kg)
$\dot{m}$	Mass flow rate (kg/s)
P	Pressure
R	Specific gas constant
R	Uncertainty function
RH, φ	Relative humidity
SI	Sustainability index
s	Specific entropy
T	Temperature (°C)
V	Air velocity (m/s)
W_n	Uncertainties in the independent variables
W_R	Total uncertainty (%)
w	Dimensional function
η	Efficiency (%)
ω	Specific humidity

Subscripts

a	Air
ch	Chemical
dest	Destruction
in	Inlet
kn	Kinetic
me	Mechanical
out	Outlet
ph	Physical
pt	Potential
v	Water vapor
Q	Heat
w	Water
wb	wet bulb
0	Dead state

1. Introduction

Forty percent of the primary energy consumption is consumed in buildings [11,34,36]. A significant portion of this energy consumption is used for heating, cooling, and air conditioning [17,27,32]. The demand for efficient use of energy in heating, ventilation, and heating (HVAC) systems in buildings increases because of the high-energy consumption in buildings [7,13,15]. In addition, evaporative cooling systems can be a pre-cooler or can be used as an economical alternative in conventional systems [1]. In addition, they are widely used systems due to zero pollution, low electrical energy consumption, and easy maintenance [4,12,35]. Evaporative cooling systems consist of two groups as the direct evaporative cooling (DEC) system and indirect evaporative cooling (IEC) system [18,31].

DEC system is an adiabatic cooling process in which sensible heat is converted into latent heat, where the enthalpy remains constant, the specific and relative humidity increases, and the dry bulb temperature decreases. Via a DEC system, the hot outside air passes over a wet porous pad. The hot air is absorbed by the water as it evaporates in the porous wet pad environment, so the air leaves the system at a lower temperature. It is an adiabatic saturation process where the dry bulb temperature decreases as the humidity of the air increases. The air transfers some of its sensible heat to the water and evaporates the water to become latent heat. Latent heat follows the water vapor and is dissipated into the air. The minimum temperature that can be obtained is the wet-bulb temperature of the incoming air [19,30].

IEC system, which is another type of evaporative cooling, has a low energy cost and high potential to meet the air conditioning demand [20]. There are two types of air passages in the system, dry and wet. In the first case, the air is perceptibly cooled without adding water. In the second case, secondary air and water flow through the second line. The surfaces of the second line are wetted with spray water so that the water evaporates into the air and the temperature of the surface is lowered. As a result, cold surfaces remove heat from outside air passing through the primary line. Thus, the air leaving the primary line has a lower dry and wet bulb temperature than the incoming air [2,14].

Exergy analysis is applied using the second law of thermodynamics to increase the efficiency of energy resource use. Exergy helps detect very large losses and achieve meaningful efficiencies. The exergy method is applied in many energy systems, including air conditioning systems. It is important to know efficient cooling techniques to evaluate alternatives or to choose the appropriate air conditioning system. Even if energy analysis was made for air conditioning systems, applying the exergy analysis is a more appropriate method. Energy analysis alone is not sufficient in a system [24]. Exergy analysis calculates the reversible work of a thermodynamic process. It helps air conditioning system manufacturers improve their systems by comparing the energy consumption of system designs with the calculated minimum energy. Studies related to exergy analysis of evaporative cooling systems are given in Table 1.

There are few studies on the exergy analysis of evaporative cooling systems in the literature. Therefore, in this study, it is aimed to directly perform the exergy analysis of an evaporative cooling system. Unlike the literature, the heat of the heated water in this system is discharged to the soil by a ground source heat exchanger. The water sprayed on the pad in the area absorbs sensible heat from the air and evaporates the water. Therefore, latent heat gain is provided to the air. The sensible heat drawn from the air by means of the pulverized water is thrown to the soil through the heat exchanger. In this way, the temperature of the water sent to the pad is subjected to a pre-cooling process. In this study, exergy efficiency and exergy destruction of a direct evaporative cooling system were evaluated over the exergy balance in four different cases. Completion of all the experiments in this study and all the steps until reaching a conclusion are given in the flow chart in Fig. 1.

Table 1
Summary of previous works related to exergy analysis of evaporative cooling systems.

Author (s)	Cooling Technique	Operating Conditions	Remarks
[14]	DEC-IEC-DEC/IEC	$T_{a,in}$: 32–42.4 °C RH_0: 19.5–67%	✓ Exergy efficiencies are between 11% and 62%.
[28]	IEC	$T_{a,in}$: 0–30 °C ω_{in}: 15.4–22.22 g/kg $\dot{m}_a$: 0.64 kg/s	✓ The exergy efficiencies are between 25% and 56%. ✓ Sustainability index decreased from 2.29 to 1.34.
[25]	IEC	$T_{a,in}$: 30–40 °C ω_{in}: 14.2–21.5 g/kg	✓ The exergy efficiency varies from 28.5% to 70%.
[22]	IEC	$T_{a,in}$: 25–45 °C RH_0: 8–18% V_{air}: 1–3 m/s	✓ The exergy efficiency is 42%. ✓ Exergy destruction is 11.5 W.
[23]	DEC	$T_{a,in}$: 28 °C RH_0: 68% V_{air}: 0.2–2.7 m/s	✓ The maximum cooling efficiency is 80.5%. ✓ The exergy efficiencies vary between 70% and 94%
[10]	DEC	$T_{a,in}$: 35.39–41.75 °C ω_{in}: 12.10–24.05 g/kg RH_0: 22.17–54.43%	✓ The energy saving rate is between 5.18% and 7.39%.
[37]	DEC/IEC	$T_{a,in}$: 18–26 °C ω_{in}: 12.6 g/kg $\dot{m}_a$: 1 kg/s	✓ Exergy efficiency increased from 55% to 88%. ✓ Exergy destruction changes between 50 W and 100 W.
[33]	IEC	$T_{a,in}$: 33.5 °C ω_{in}: 8.24 g/kg V_{air}: 1.5 m/s	✓ The exergy efficiency is obtained 59.2%. ✓ Exergy destruction changes between 20 W and 150 W.
[24]	DEC	$T_{a,in}$: 30–50 °C $\dot{m}_w$: 0.0465–0.1667 kg/s V_{air}: 1–3 m/s	✓ Cooling efficiency is obtained as 84%. ✓ The overall exergy is determined as 74%.
[16]	IEC	$T_{a,in}$: 30–40 °C ω_{in}: 8.45 g/kg V_{air}: 2 m/s	✓ According to different configurations, the exergy efficiencies are 19.69% and 74.32%. ✓ Exergy destruction changes between 119 W and 180.4 W. ✓ Sustainability index are between 4.8 and 7.282.
[31]	IEC	T_{amb}: 26–40 °C ω_{amb}: 5–20 g/kg $\dot{m}_a$: 0.1–0.3 kg/s	✓ The exergy efficiency ranges from 19.7% to 22.7%. ✓ The energy saving rate reached 48.6%. ✓ Cooling efficiencies changes between 67.1% and 89%.

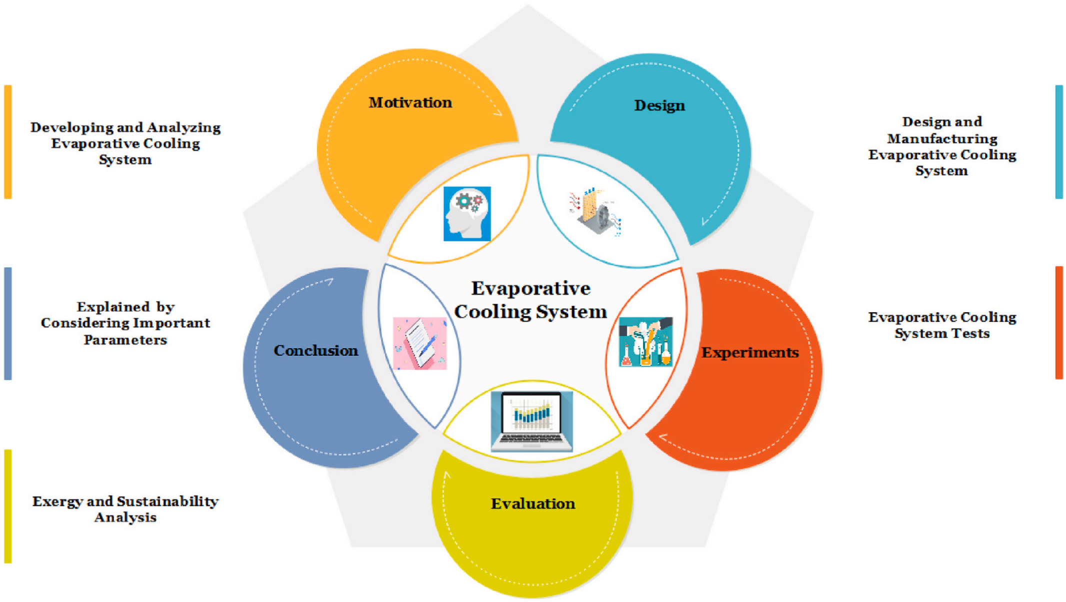

Fig. 1. Flow chart of evaporative cooling system.

2. Material and methods

2.1. Experimental setup

In this study, an evaporative cooling system with a cooling pad was designed and manufactured. The ground source evaporative cooling system is given in Fig. 2. The difference in the evaporative cooling system compared to many studies in the literature is that there is a heat exchanger located under the ground. The system consists of three main parts as cooling water circulation line, a ground

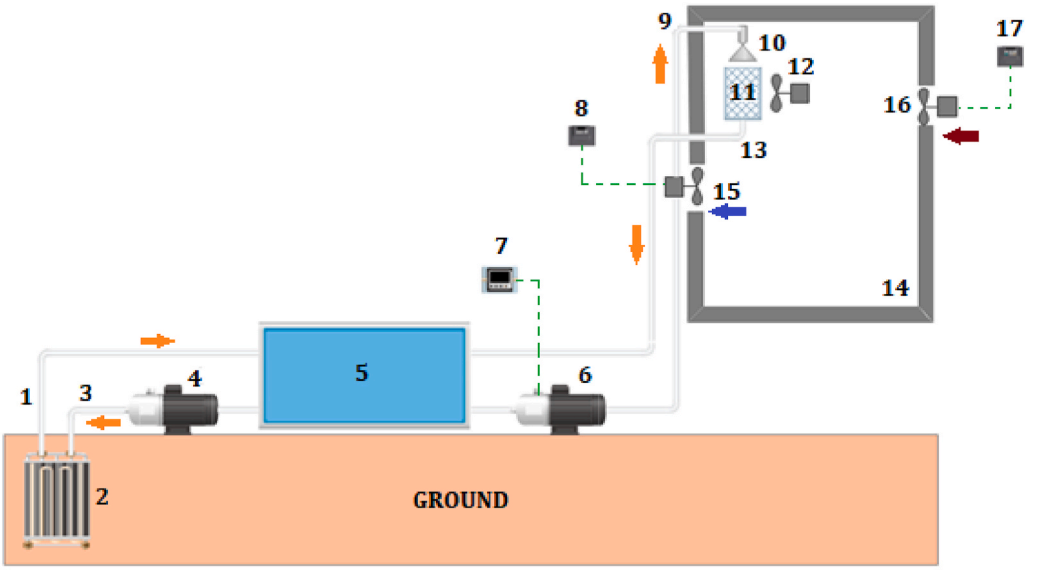

1	Ground return line	7	Control card (timer)	13	Cooling pad drainage line
2	Heat exchanger	8 and 17	Fan speed controller	14	Room
3	Ground input line	9	Cooling pad supply line	15	Exhaust fan
4	Circulation pump	10	Cooling pad nozzles	16	Fresh air fan
5	Water tank	11	Cooling pad		
6	Circulation pump for cooling pad	12	Cooling fans (3 numbers)		

Fig. 2. View of ground source evaporative cooling system.

source line, and a cooling pad line. The circulation of the water passed through the heat exchanger buried in the ground is provided by a pump (Number 4 in Fig. 2). The water passed through the ground source heat exchanger is collected in an insulated water tank (Number 5 in Fig. 2). The cooling pad line, which is the second line in the system, is circulated by a second pump. The control of this circulation pump is adjusted to operate for 4 min with the control card (timer) (Number 7 in Fig. 2) and is interrupted for 1 min. The cold water from the pump is sent to the cooling pad via the pipeline. The water coming to the cooling pad is transferred to the cooling pad with the help of pulverized nozzles. At this time, cooling is carried out with the cooling fans. In this process, when small droplets of water are sent into the unsaturated air, these water droplets evaporate. Depending on the evaporation, the sensible heat of the ambient air turns into latent heat with the evaporation of the water. The dry bulb temperature drops due to the reduced sensible heat of the ambient air. In addition, the cold water flowing over the cooling pad is drained and stored again. In order to keep the humidity in the cooled room between 50 and 60%, fresh air is taken with one of the fans in the room and the air inside is given out with the other fan.

Since the experiments were carried out at different air velocities, a DC fan speed controller (Number 8 and 17 in Fig. 2) was operated for two different air velocity conditions to adjust the air velocity. The different operating conditions applied in the experiments are given in Table 2.

A timer (7 number in Fig. 2) is used for water pulverizing equipment. The energy needed for the system was obtained from a 12 V power supply. The equipment used in the system is given in Table 3. An electronic circuit was prepared for the designed and manufactured evaporative cooling system. The circuit performs automatic control so that the water does not flow continuously. Pumping the water in the system takes 4 min. After this period, the pumps are stopped for 1 min so that the relative humidity of the environment does not increase. Meanwhile, the fans dry the surface of the cooling pad.

The representation of the points where the measurements made in the system during the experiments were taken are given in Fig. 3.

2.2. Uncertainty analysis

The total uncertainty analysis of the ground source evaporative cooling system in this experimental study was calculated in Equation (1). In the equation, W_R is the total uncertainty of the system (%), R and w are the uncertainty function and dimensional factor, respectively. In this equation, w_n represents the uncertainties in the independent variables [9,26]. The characteristics of all measurement instruments used in the evaporative cooling system are given in Table 4.

$$W_R = \left[\left(\frac{\partial R}{\partial x_1} w_1\right)^2 + \left(\frac{\partial R}{\partial x_2} w_2\right)^2 + \ldots + \left(\frac{\partial R}{\partial x_n} w_n\right)^2\right]^{1/2} \tag{1}$$

Accordingly, the uncertainty value is calculated to be 1.79% for relative humidity, 2.892% for ambient temperature, 3.235% for room temperature, 1.271% for energy consumption, 2% for fresh air velocity, 1.739% for exhaust air velocity, and 1.923% for ground temperature. Accordingly, the overall uncertainty value of the experimental rig is found to be 4.5%.

2.3. Thermodynamic modelling

The work potential of a system under certain conditions can be evaluated by allowing the system to move towards and reach a stable equilibrium with the environment. In reality, when the system and environmental conditions reach equilibrium, another state change does not occur spontaneously. When such a situation occurs, it is considered the dead state of the system. Since the initial temperature of the heat transfer fluid in the evaporative cooling system is the same as the ambient temperature (T_0), the initial exergy is zero. In addition, the specific humidity value (ω_0) for the dead state is also the value corresponding to this temperature.

Exergy analysis is of great importance in systems that generate thermal energy and rely on the second law of thermodynamics. The exergy balance equations of the ground source evaporative cooling system shown in Fig. 2 are given below.

Total exergy of a system consists of four parameters: physical exergy ($\dot{E}x^{ph}$), potential exergy ($\dot{E}x^{pt}$), kinetic exergy ($\dot{E}x^{kn}$) and chemical exergy ($\dot{E}x^{ch}$).

$$\dot{E}x = \dot{E}x^{ph} + \dot{E}x^{kn} + \dot{E}x^{pt} + \dot{E}x^{ch} \tag{2}$$

The total specific exergy on a mass basis in a system is as follows:

$$ex = ex^{ph} + ex^{kn} + ex^{pt} + ex^{ch} \tag{3}$$

The general exergy equation can be given as:

Table 2
The explanation of cases in the experiments (air density is accepted as 1.2 kg/m^3 in mass flow calculations).

Case 1 (Negative pressure)	Fresh air properties (air velocity, volumetric flow rate, and mass flow rate)	1 m/s, 0.0144 m^3/s, 0.01728 kg/s
	Exhaust air properties (air velocity, volumetric flow rate, and mass flow rate)	1.3 m/s, 0.01872 m^3/s, 0.0224 kg/s
Case 2 (Negative pressure)	Fresh air properties (air velocity, volumetric flow rate, and mass flow rate)	2 m/s, 0.0288 m^3/s, 0.0345 kg/s
	Exhaust air properties (air velocity, volumetric flow rate, and mass flow rate)	2.3 m/s, 0.03312 m^3/s, 0.0397 kg/s
Case 3 (Positive pressure)	Fresh air properties (air velocity, volumetric flow rate, and mass flow rate)	1.3 m/s, 0.01872 m^3/s, 0.0224 kg/s
	Exhaust air properties (air velocity, volumetric flow rate, and mass flow rate)	1 m/s, 0.0144 m^3/s, 0.01728 kg/s
Case 4 (Positive pressure)	Fresh air properties (air velocity, volumetric flow rate, and mass flow rate)	2.3 m/s, 0.03312 m^3/s, 0.0397 kg/s
	Exhaust air properties (air velocity, volumetric flow rate, and mass flow rate)	2 m/s, 0.0288 m^3/s, 0.0345 kg/s

Table 3
Specifications of components in the evaporative cooling system.

Components	Specifications
Test room	0.25 m^3
Circulation pumps	6 bar, DC
Cooling pad	10 × 15 × 50 cm
System control card (timer)	12 VDC
Power Supply	12 V, 15 A, 180 W
Heat exchanger	1/4 - 3/4 HP
Fan speed controller	12 VDC
Fans	12 VDC, 0.25 A, 120 mm × 120 mm

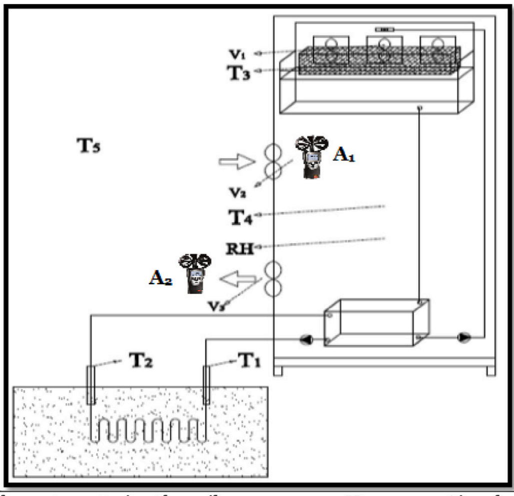

T_1	Temperature of the water entering the soil	V_1	Air velocity behind pad
T_2	Temperature of the water leaving the soil	V_2	Fresh air velocity
T_3	Temperature of the air at the exit of the pad	V_3	Exhaust air velocity
T_4	Room temperature	RH	Measurement of relative humidity
T_5	Ambient temperature	A1-A2	Anemometers

Fig. 3. Measuring points from which experimental data were taken.

Table 4
Specifications of measurement devices in the evaporative cooling system.

Device	Specifications
Temperature measuring device	4 Channel, K Temperature Range: −200–1370 °C, K Temperature Accuracy: ± (0.3% rdg+1 °C), K Temperature Resolution: 0.1 °C
Thermohygrometer	Temperature – NTC Measuring range: 10 to ~60 °C Accuracy: ±0.5 °C Resolution: 0.1 °C Humidity – Capacitive Measuring range: 0–100 %RH Accuracy: ±2.5 %RH (5–95 %RH) Resolution: 0.1 %RH
Anemometer	Measurement range: 0.1–40 m/s Accuracy: ±0.4 m/s (1.00–9.99 m/s) Resolution: 0.01 m/s
Power meter	Mains voltage input: 220–240 VAC Load limit: 3680 W

$$\sum \dot{E}x_{in} - \sum \dot{E}x_{out} = \sum \dot{E}x_{dest} \tag{4}$$

In Equation (5), the potential and kinetic energies are considered to be negligible. $\dot{E}x_Q$ is the exergy related to heat transfer. $\dot{E}x_{dest}$ is exergy destruction, which is a positive amount for any real process and zero for a reversible process. *ex* represents specific exergy as seen in Equation (7).

$$\sum_{in} Ex_Q + \sum_{in} m(ex) - \sum_{out} Ex_Q - \sum_{out} m(ex) - Ex_{dest} = 0 \tag{5}$$

$$\dot{E}x_Q = \sum \left(1 - \frac{T}{T_0}\right)\dot{Q} \tag{6}$$

$$ex = (h - h_0) - T_0(s - s_0) \tag{7}$$

The total work potential of a fluid is defined as the flow exergy. The flow exergy of moist air is calculated based on the state characteristics (T, ω, P) and relative to the dead state (T_0, ω_0, P_0, φ_0): thermal, mechanical, and chemical exergy [8]. The specific exergy equations for these three terms are as follows [22]. ex_{me} expression includes fan and pump.

$$ex_a = ex_{th} + ex_{me} + ex_{ch} \tag{8}$$

$$ex_{th} = (c_{pa} + \omega c_{pv}) T_0 \left(\frac{T}{T_0} - 1 - ln\frac{T}{T_0}\right) \tag{9}$$

$$ex_{me} = (1 + 1.608\omega) R_a T_0 ln\frac{P}{P_0} \tag{10}$$

$$ex_{ch} = R_a T_0 \left[(1 + 1.608\omega) ln\frac{1 + 1.608\omega_0}{1 + 1.608\omega} + 1.608\omega ln\frac{\omega}{\omega_0}\right] \tag{11}$$

where, c_{pa} is air specific heat at constant pressure, c_{pv} is water vapor specific heat at constant pressure, R_a is the air specific gas constant

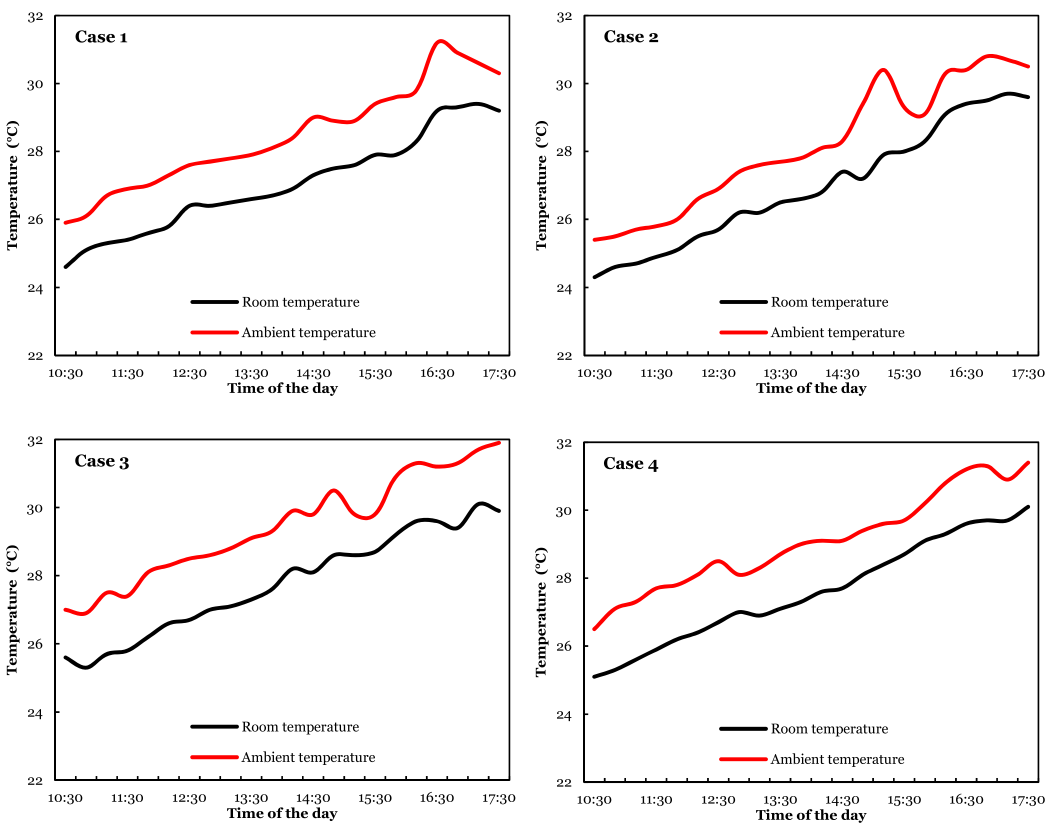

Fig. 4. Change of ambient temperature and room temperature with time.

and the constant 1.608 is the ratio of the molar mass of air to the molar mass of water vapor. The specific exergy of liquid water can be calculated in equation (10) below.

$$ex_w = -R_v T_0 ln\varphi_0 \tag{12}$$

where, R_v is water vapor gas constant and φ_0 relative humidity at dead state. The exergy efficiency of the evaporative cooling system can be calculated as in Equation (12).

$$\eta_{ex} = \frac{ex_{a2}}{ex_{a1} + (\omega_2 - \omega_1)ex_w} \tag{13}$$

The cooling efficiency for ground source evaporative cooling system can be calculated according to the following equation [5,6]:

$$\eta_{ce} = \frac{(T_1 - T_2)}{(T_1 - T_{wb})} \tag{14}$$

Van Gool suggested that the maximum improvement in exergy efficiency for a process or system is achieved when exergy loss or irreversibility is minimized. As a result, he argued that it would be beneficial to use an exergetic concept of improvement potential (EIP) when performing system analysis [29]. The improvement potential equation is given as:

$$EIP = (1 - \eta_{ex})(ex_{in} - ex_{out}) \tag{15}$$

Exergy analysis provides an opportunity to improve the performance of a system. The sustainability index is another parameter that gives an idea of how exergy efficiency affects the sustainability of resources or systems. It is directly related to the exergy efficiency. Therefore, it represents how important exergy methods are in increasing the efficiency of the system [3].

$$SI = \frac{1}{1 - \eta_{ex}} \tag{16}$$

3. Results and discussions

The data obtained as a result of detailed experimental analyzes in the evaporative cooling system are presented in this section. Firstly, as seen in Fig. 4, the room and ambient temperature for each case are shown graphically. Since the ambient temperature changed during the period of the experiments, room temperatures also changed. In this situation, the most accurate way is to observe the variation of the two temperatures in parallel. Thus, the cooling efficiency for each case can be better analyzed. In direct evaporative cooling systems, it is expected that the ambient temperature will decrease as the humidity of the air increases. This is due to the transfer of the sensible heat of the air to the water [21]. The opposite of this situation is seen in Figs. 3 and 4. As the humidity of the room air decreases with time, the room temperature increases. Here, the increase in room temperature causes the amount of humidity in the air to decrease, which causes the air to give less sensible heat to the water.

As explained in the previous sections, the sensible heat in the room is converted into latent heat in the adiabatic cooling process. In this way, the temperature of the room is lowered and the relative humidity is increased, and accordingly, the specific humidity of the environment increases at the same time. Relative humidity changes in the room and ambient are given in Fig. 5. When four different cases are examined, the biggest difference between relative humidity is seen in case 3. As seen in Fig. 8 (b), the relative humidity increases when the temperature difference is high. According to Fig. 5, the average relative humidity values in the room were determined for each case. Accordingly, the average relative humidity values were determined as 68.82%, 62.91%, 70.73% and 68.81%, respectively. Thus, according to the obtained average relative humidity values, it is easily understood that the situation with the most adiabatic cooling is case 3. Because high relative humidity means a decrease in temperature. For this reason, the best cooling efficiency performance will be obtained from the evaporative cooling system.

In Fig. 6, the average exergy efficiency and exergy losses for each case are seen. Exergy efficiencies were determined as 16.8% for case 1, 17.5% for case 2, 20.8% for case 3 and 18.4% for case 4. In addition, exergy losses are calculated as 73, 100, 80, and 73 J/kg, respectively, and presented graphically. In case 3 where the ambient temperature is the highest, the room temperature is approximately the same as in the other three cases, so the cooling in the room is noticeably better in case 3. Parallel to this situation, the exergy efficiency was at the highest values for case 3. However, considering the exergy losses, the lowest loss value is not in case 3. The reason for this can be defined as the increased ambient air temperature causing more losses. Despite this situation, the loss values are very close to case 1 and case 4.

When looking at Fig. 7, the change in sustainability and EIP values can be seen. It is seen that the sustainability value (a) is the highest in case 3, followed by case 4, case 2, and case 1, respectively. Sustainability value generally shows parallelism with exergy efficiency. When the EIP value (b) is examined, it is observed that this value occurs in similar curves with the exergy loss values. Considering these situations, it was determined that the exergy efficiency gives much clearer information about both the usability and sustainability of the system. The Case 3 system is the system in which the possibilities of doing business are evaluated in the best way compared to the systems in other cases. However, it still has losses and exergy improvement potential. When these improvements are made, the usability of the system will reach higher values.

In Fig. 8, the variation of the cooling efficiency (a) and the difference between ambient air temperature and room temperature (b) are seen for each case. The average temperature difference is 1.45 °C for case 1, 1.21 °C for case 2, 1.6 °C for case 3 and 1.48 °C for case 4, respectively. The highest cooling efficiency was observed in case 3 with 41%, followed by case 4 with 37%, case 2 with 35%, and

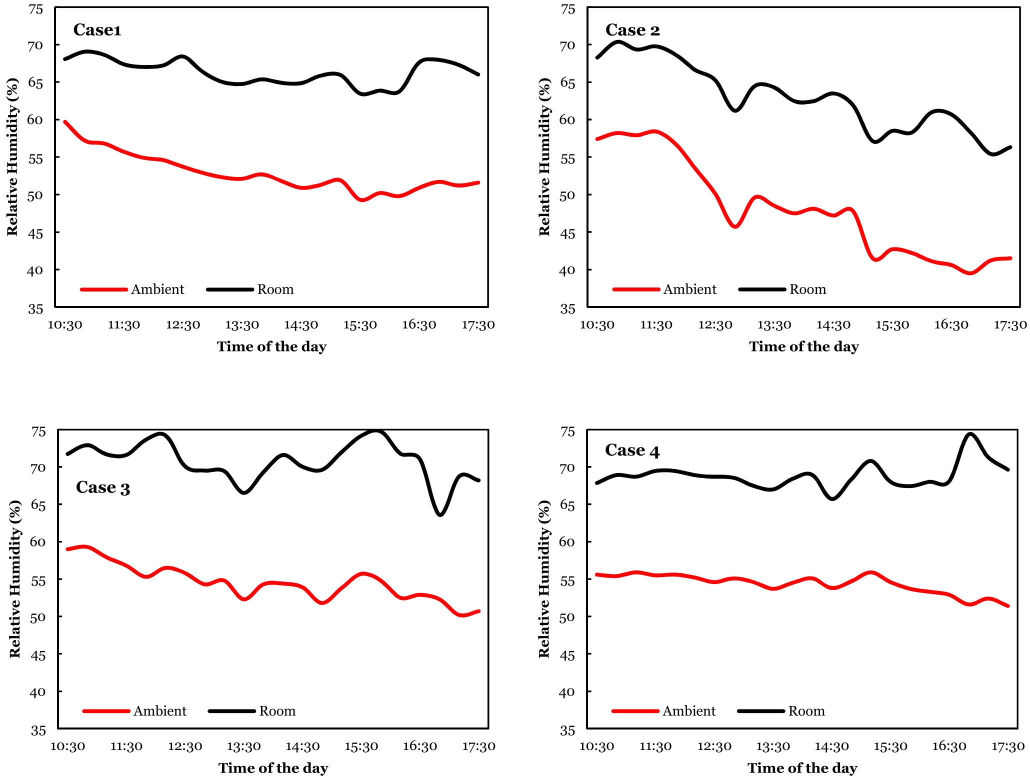

Fig. 5. Changes of ambient relative humidity and room relative humidity over time.

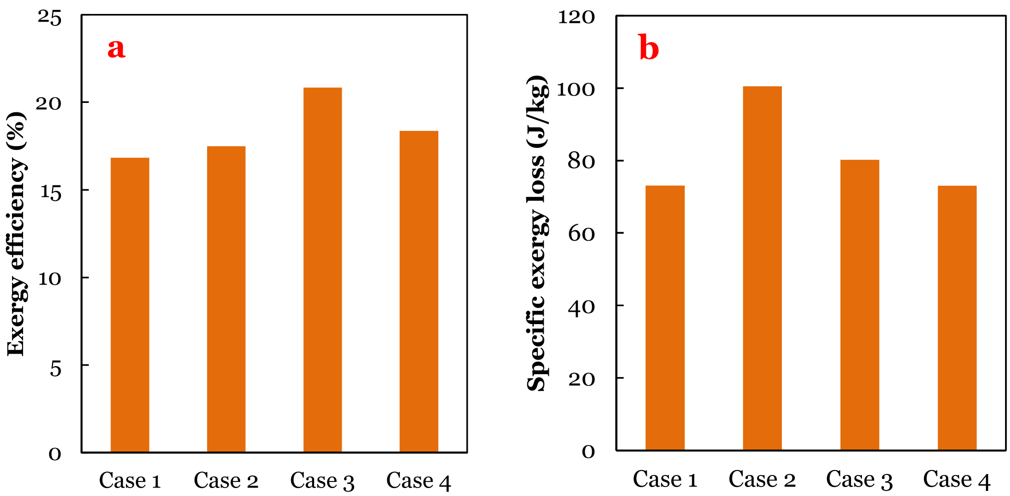

Fig. 6. Average exergy efficiency (a) and average exergy loss (b).

case 1 with 33%. The cooling efficiency of the system can be observed most ideally by detecting the difference between indoor and outdoor temperatures. In this situation, as seen in Fig. 8 (b), the highest difference was found in case 3. The graphs examined so far clearly show us that the best system is case 3. The Case 3 system operates between 12% and 19% more effectively than other systems.

Fig. 9 includes a performance review method presented for the first time in this study. This figure shows approximately how much energy should be consumed to cool each 1 °C, and this parameter is very important for air conditioning systems. This figure clearly shows us that the ideal cooling process takes place in case 3. Compared to the average of other systems, the case 3 system consumes

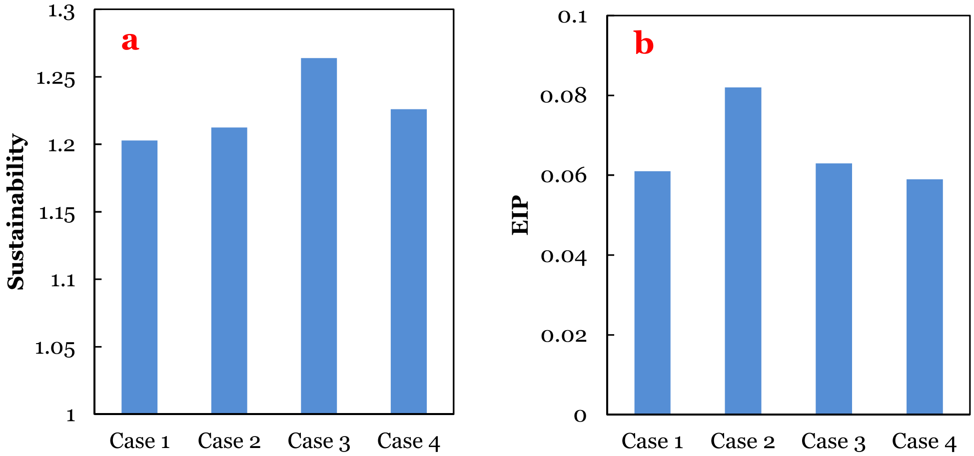

Fig. 7. Sustainability (a) and exergetic improvement potential (b).

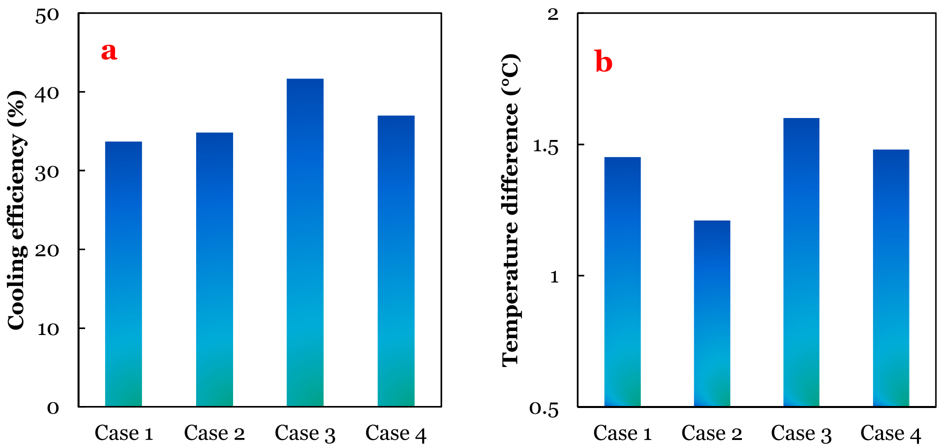

Fig. 8. Average cooling efficiency (a) and average temperature difference between room and ambient temperature (b).

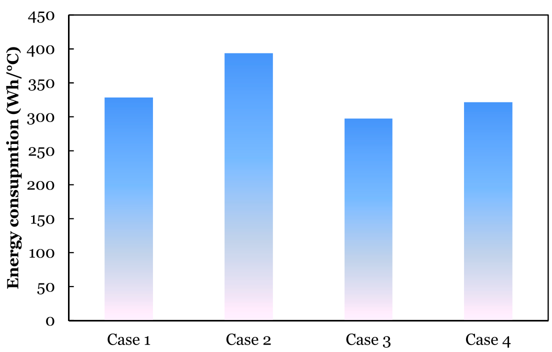

Fig. 9. Energy consumption for each cases.

approximately 15% less energy and performs the cooling process.

The psychrometric analysis of the ground source evaporative cooling system for each case is given in Fig. 10. Point 1 in the figure represents the air in the room. In order to maintain the humidity balance in the room and prevent the relative humidity from increasing

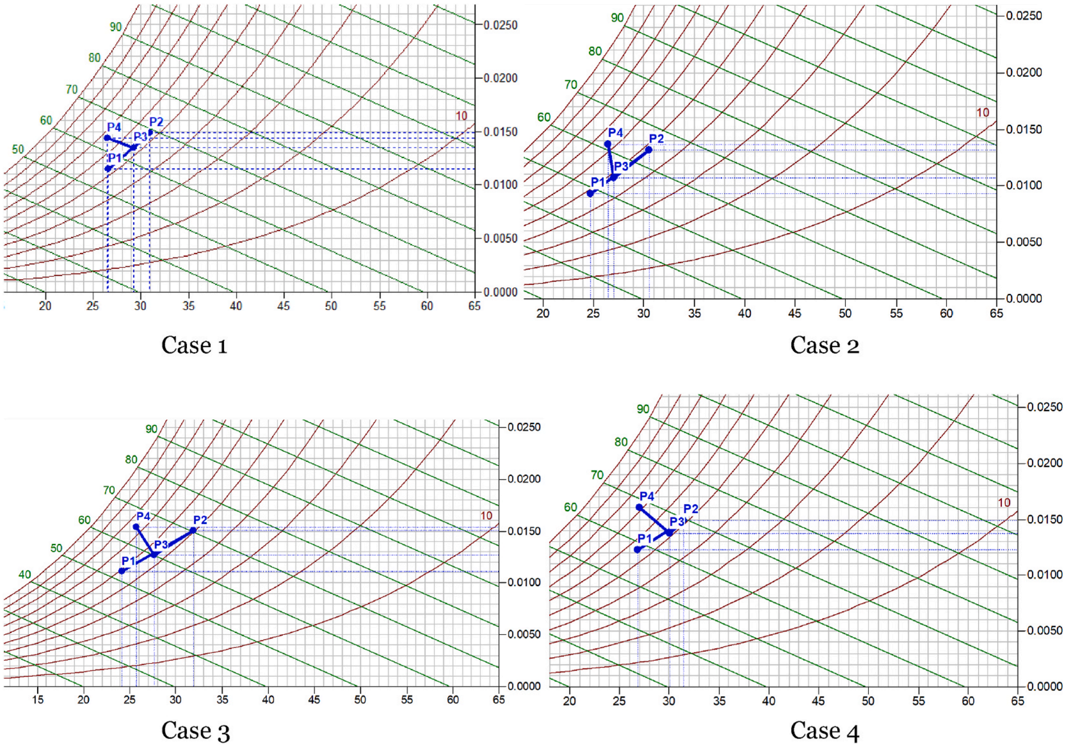

Fig. 10. Psychrometric analysis of the evaporative cooling system for each case.

significantly, the air is expelled from the room by means of a fan. Point 2 shows the air taken from outside. In order to maintain the humidity balance, the same amount of outside air is taken in as the expelled air. Point 3 is mixed air, that is, cooling pad inlet air. Evaporative cooling takes place at point 4. Since the air inside the cooling pad is mixed with the room air and comes out of the point 4 that are thrown out, the relative humidity at point 1 did not rise. In order to provide positive pressure inside, air is taken from outside instead of exhausted air in point 2 number conditions. The opposite is true for negative pressure. While the air at point 4 is exposed to constant specific humidity and sensible heat gain with outdoor air gains in the dotted line point 4, this air has reached the point 1 point with specific humidity loss. This situation occurs as a result of expelling the moist air from the inside at a certain rate.

4. Conclusion

In this study, an evaporative cooling system was examined experimentally for 4 different cases and the results were analyzed. Cases called case 1 and case 2 have a negative airflow, while case 3 and case 4 have a positive airflow. As a result of detailed analysis, the following results were obtained.

- Positive pressure systems work more efficiently than negative pressure systems. However, this study shows us that it is very important to be able to balance the fresh air taken and the exhaust air in the places to be air-conditioned. Although the case 4 has positive pressure, it has almost the same values as case 2 and case 1. With 1.3–1 m/s air velocities in Case 3, it is seen as the most ideal pressurization system in this study.
- The highest exergy efficiency was obtained in case 3 as 20.8%. The exergy efficiency is inversely proportional to the temperature. As the temperature increased, the exergy efficiency decreased. In this study, temperature and temperature differences are given in the previous sections. Therefore, while the exergy efficiency will be highest in the case with the highest temperature difference, the exergy efficiency will be the lowest in the lowest case. Considering the temperature differences between the cases, the highest temperature difference with 1.6 °C is case 3. Therefore, case 3 has the highest exergy efficiency. The temperature difference in other cases is 1.45 °C for case 1, 1.21 °C for case 2 and 1.48 °C for case 4, respectively. According to these temperature differences, exergy efficiencies were determined as 16.8%, 17.5% and 18.4%, respectively.
- Sustainability and EIP are important parameters for the usability of a system. Sustainability and EIP are parallel to the ratios in exergy efficiency. For example, in case 3, where the exergy efficiency is 20.8%, the sustainability index is 1.26. However, the EIP value is higher than case 1 and case 4, which have low exergy efficiencies, and it is seen that there is still a need for improvement.
- Case 3 has the highest cooling efficiency with 41%. The reason for this can be explained as giving more sensible heat to the air and absorbing more latent heat. This can also be seen from temperature differences. The best adiabatic cooling is achieved when the ambient temperature is reduced as much as possible and the relative humidity of the air is increased.

- Energy consumption is one of the important issues today. For this, many energy saving studies and system improvements are made. It is a great advantage that the evaporative cooling system in this study has low energy consumption. For four different cases implemented in the system, case 3 consumed 9.38% less energy than case 1, 24.37% less than case 2 and 7.5% less energy than case 4. As a result, case 3 requires approximately 15% more energy to cool the system by 1 °C compared to other cases.
- It was determined that while exergy efficiency and cooling efficiency increase under negative pressure at high air speed, it decreases under positive pressure.

Author statement

Gökhan Yıldız: Conceptualization, Methodology, Investigation, Writing - Original Draft, Writing - Review & Editing, Visualization. **Alper Ergün:** Conceptualization, Methodology, Investigation, Writing - Original Draft, Writing - Review & Editing, Visualization. **Ali Etem Gürel:** Conceptualization, Methodology, Investigation, Writing - Original Draft, Writing - Review & Editing, Visualization. Supervisor. **İlhan Ceylan:** Conceptualization, Methodology, Investigation, Writing - Original Draft, Writing - Review & Editing, Visualization. **Ümit Ağbulut:** Conceptualization, Methodology, Investigation, Writing - Original Draft, Writing - Review & Editing, Visualization. **Servet Eser:** Conceptualization, Methodology, Investigation, Writing - Original Draft. **Asif Afzal:** Conceptualization, Methodology, Investigation, Writing - Original Draft. **C Ahamed Saleel:** Conceptualization, Methodology, Investigation, Writing - Original Draft.

Declaration of competing interest

The authors declare that they have no known competing financial interests or personal relationships that could have appeared to influence the work reported in this paper.

Acknowledgment

The authors extend their appreciation to the Deanship of Scientific Research at King Khalid University, Saudi Arabia for funding this work through the General Research Project under Grant No: GRP/171/43 .

References

[1] F.M. Abed, M.H. Zaidan, M. Hasanuzzaman, L. Kumar, A.K. Jasim, Modelling and experimental performance investigation of a transpired solar collector and underground heat exchanger assisted hybrid evaporative cooling system, J. Build. Eng. 44 (2021), 102620.
[2] J.S.J. Alonso, F.R. Martinez, E.V. Gomez, M.A.G. Plasencia, Simulation model of an indirect evaporative cooler, Energy Build. 29 (1) (1998) 23–27.
[3] H. Çaliskan, I. Dincer, A. Hepbasli, Energy, exergy and sustainability analyses of hybrid renewable energy based hydrogen and electricity production and storage systems: modeling and case study, Appl. Therm. Eng. 61 (2) (2013) 784–798.
[4] J.R. Camargo, C.D. Ebinuma, J.L. Silveira, Experimental performance of a direct evaporative cooler operating during summer in a Brazilian city, Int. J. Refrig. 28 (7) (2005) 1124–1132.
[5] A. Çaylı, A. Akyüz, S. Üstün, B. Yeter, Efficiency of two different types of evaporative cooling systems in broiler houses in Eastern Mediterranean climate conditions, Therm. Sci. Eng. Prog. 22 (2021), 100844.
[6] İ. Ceylan, A. Ergün, B. Acar, M. Aydin, Psychometric and thermodynamic analysis of new ground source evaporative cooling system, Energy Build. 119 (2016) 20–27.
[7] İ. Ceylan, G. Yildiz, A.E. Gürel, A. Ergün, A. Tosun, The effect of malfunctions in air handling units on energy and exergy efficiency, Heat Tran. Res. 51 (11) (2020) 1007–1028.
[8] R. Chengqin, L. Nianping, T. Guangfa, Principles of exergy analysis in HVAC and evaluation of evaporative cooling schemes, Build. Environ. 37 (11) (2002) 1045–1055.
[9] Z. Cingiz, F. Katırcıoğlu, S. Sarıdemir, G. Yıldız, Y. Çay, Experimental investigation of the effects of different refrigerants used in the refrigeration system on compressor vibrations and noise, International Advanced Researches and Engineering Journal 5 (2) (2021) 152–162.
[10] A.K. Dhamneya, S.P.S. Rajput, A. Singh, Theoretical performance analysis of window air conditioner combined with evaporative cooling for better indoor thermal comfort and energy saving, J. Build. Eng. 17 (2018) 52–64.
[11] P.A. Doğramacı, D. Aydın, Comparative experimental investigation of novel organic materials for direct evaporative cooling applications in hot-dry climate, J. Build. Eng. 30 (2020), 101240.
[12] Z. Duan, X. Zhao, J. Liu, Q. Zhang, Dynamic simulation of a hybrid dew point evaporative cooler and vapour compression refrigerated system for a building using EnergyPlus, J. Build. Eng. 21 (2019) 287–301.
[13] M. El Loubani, N. Ghaddar, K. Ghali, M. Itani, Hybrid cooling system integrating PCM-desiccant dehumidification and personal evaporative cooling for hot and humid climates, J. Build. Eng. 33 (2021), 101580.
[14] M. Farmahini-Farahani, S. Delfani, J. Esmaeelian, Exergy analysis of evaporative cooling to select the optimum system in diverse climates, Energy 40 (1) (2012) 250–257.
[15] G. Heidarinejad, M.F. Farahani, S. Delfani, Investigation of a hybrid system of nocturnal radiative cooling and direct evaporative cooling, Build. Environ. 45 (6) (2010) 1521–1528.
[16] S. Kashyap, J. Sarkar, A. Kumar, Exergy, economic, environmental and sustainability analyses of possible regenerative evaporative cooling device topologies, Build. Environ. 180 (2020), 107033.
[17] S. Kashyap, J. Sarkar, A. Kumar, Performance enhancement of regenerative evaporative cooler by surface alterations and using ternary hybrid nanofluids, Energy 225 (2021), 120199.
[18] S. Kashyap, J. Sarkar, A. Kumar, Effect of surface modifications and using hybrid nanofluids on energy-exergy performance of regenerative evaporative cooler, Build. Environ. 189 (2021), 107507.
[19] S. Kashyap, J. Sarkar, A. Kumar, Experimental exergy, economic and sustainability analyses of the dual-mode evaporative cooler, Int. J. Refrig. (2021), https://doi.org/10.1016/j.ijrefrig.2021.12.005. In Press.
[20] P. Kowalski, D. Kwiecień, Evaluation of simple evaporative cooling systems in an industrial building in Poland, J. Build. Eng. 32 (2020), 101555.
[21] A. Laknizi, M. Mahdaoui, A.B. Abdellah, K. Anoune, M. Bakhouya, H. Ezbakhe, Performance analysis and optimal parameters of a direct evaporative pad cooling system under the climate conditions of Morocco, Case Stud. Therm. Eng. 13 (2019), 100362.
[22] J. Lin, D.T. Bui, R. Wang, K.J. Chua, On the exergy analysis of the counter-flow dew point evaporative cooler, Energy 165 (2018) 958–971.
[23] P. Martínez, J. Ruiz, P.J. Martínez, A.S. Kaiser, M.J.A.T.E. Lucas, Experimental study of the energy and exergy performance of a plastic mesh evaporative pad used in air conditioning applications, Appl. Therm. Eng. 138 (2018) 675–685.

[24] S.A. Nada, A. Fouda, M.A. Mahmoud, H.F. Elattar, Experimental investigation of energy and exergy performance of a direct evaporative cooler using a new pad type, Energy Build. 203 (2019), 109449.
[25] D. Peng, J. Zhou, D. Luo, Exergy analysis of a liquid desiccant evaporative cooling system, Int. J. Refrig. 82 (2017) 495–508.
[26] Sarıdemir, S., Yıldız, G., & Hanedar, E. Effect of diesel-biodiesel-methanol blends on performance and combustion characteristics of diesel engine. Düzce Üniversitesi Bilim ve Teknoloji Dergis, 9(1), 189-201.
[27] B.N. Taufiq, H.H. Masjuki, T.M.I. Mahlia, M.A. Amalina, M.S. Faizul, R. Saidur, Exergy analysis of evaporative cooling for reducing energy use in a Malaysian building, Desalination 209 (1–3) (2007) 238–243.
[28] İ. Uçkan, T. Yılmaz, E. Hürdoğan, O. Büyükalaca, Exergy analysis of a novel configuration of desiccant based evaporative air conditioning system, Energy Convers. Manag. 84 (2014) 524–532.
[29] W. Van Gool, Energy policy: fairy tales and factualities, in: Innovation and Technology—Strategies and Policies, Springer, Dordrecht, 1997, pp. 93–105.
[30] Y. Yang, G. Cui, C.Q. Lan, Developments in evaporative cooling and enhanced evaporative cooling-A review, Renew. Sustain. Energy Rev. 113 (2019), 109230.
[31] Y. Yang, C. Ren, C. Yang, M. Tu, B. Luo, J. Fu, Energy and exergy performance comparison of conventional, dew point and new external-cooling indirect evaporative coolers, Energy Convers. Manag. 230 (2021), 113824.
[32] G. Yıldız, Ü. Ağbulut, A.E. Gürel, A review of stability, thermophysical properties and impact of using nanofluids on the performance of refrigeration systems, Int. J. Refrig. 129 (2021) 342–364.
[33] L. Wang, C. Zhan, J. Zhang, X. Zhao, The energy and exergy analysis on the performance of counter-flow heat and mass exchanger for M-cycle indirect evaporative cooling, Therm. Sci. 23 (2 Part A) (2019) 613–623.
[34] Z. Wang, G. Li, F. Wang, Z. Liu, M. Wang, Performance analysis and operation optimization of air-to-water CO_2 heat pump with phase change thermal storage, Energy Build. 209 (2020), 109738.
[35] J.M. Wu, X. Huang, H. Zhang, Numerical investigation on the heat and mass transfer in a direct evaporative cooler, Appl. Therm. Eng. 29 (1) (2009) 195–201.
[36] E. Zanchini, C. Naldi, Energy saving obtainable by applying a commercially available M-cycle evaporative cooling system to the air conditioning of an office building in North Italy, Energy 179 (2019) 975–988.
[37] L. Zhang, X. Zha, X. Song, X. Zhang, Optimization analysis of a hybrid fresh air handling system based on evaporative cooling and condensation dehumidification, Energy Convers. Manag. 180 (2019) 83–93.